Cell wall digestibility outperforms ear in maintaining digestibility even under severe combined water and heat stress

Oscar Main[1], Ana López-Malvar[1,2], Florence Meunier[3], Sophie Guillaume[1], Marie-Pierre Jacquemot[1], Paul-Louis Lopez-Marnet[1], Charlène Barotin[4], Anne Marmagne[1], Laurent Cézard[1], Sébastien Fargier[3], Sébastien Rey[3], Pierre Larsonneau[5], Matthieu Reymond[1], Nathalie Mangel[6], Anthony Uijttewaal[7], Sylvie Coursol[1], Valérie Méchin[1].

[1]Université Paris Saclay, INRAE, AgroParisTech, Institute Jean-Pierre Bourgin for Plant Sciences (IJPB), 78000, Versailles, France.

[2]Facultad de Biología, Departamento de Biología Vegetal y Ciencias del Suelo, Agrobiología Ambiental, Calidad de Suelos y Plantas, Universidad de Vigo, As Lagoas Marcosende, 36310 Vigo, Spain,Unidad Asociada a la Misión Biológica de Galicia (CSIC).

[3]Unité Expérimentale DiaScope, INRAE, Mauguio, France.

[4]Unité de Recherche Pluridisciplinaire, Prairies, Plantes Fourragères, INRAE, Lusignan, France.

[5]ARVALIS – Institut du végétal, Station expérimentale, Baziège, France.

[6]ARVALIS – Institut du végétal, Station expérimentale de La Jaillière, Loireauxence, France.

[7]ARVALIS – Institut du végétal, Station expérimentale, Boigneville, France.

Running title: Boost maize quality resilience with cell wall digestibility

Highlight: Under severe drought, maize digestibility is upheld by boosted cell wall digestibility, which is facilitated by a reduction in the *p*-hydroxycinnamic acid content, while the lignin content remains stable.

Abstract: Forage maize is a central pillar of dairy cow feeding in France, directly influencing milk production. Drought significantly affects both its yield and digestibility, which are essential for registration purposes. Research on inbred lines revealed droughts notable effect on dry matter and cell wall digestibilities, directly impacting forage quality. Nevertheless, further investigation is warranted due to increasing frequency of drought. To delve deeper, we grew a range of modern forage maize hybrids for two years under four different field water-monitored modalities, representing a total of eight environmental conditions. The resulting dataset allowed us to perform a multiscale analysis, integrating agroclimatic, agronomic, biochemical and histological traits. By establishing a comprehensive heat and water stress index,

we classified the environmental conditions. We demonstrated that under severe stress, ear production decreases significantly, but dry matter digestibility can be maintained through increased cell wall digestibility. This boost in cell wall digestibility was due to a reduction in *p*-hydroxycinnamic acid content, while lignin content remained relatively stable between environments. The significance of lignin distribution increased with the severity of the stress, reaching an extreme threshold where biochemical parameters solely account for digestibility variations.

Keywords: cell wall**;** digestibility**;** drought; field trials; forage maize; lignin content, structure, composition and distribution; stress index; yield.

Abbreviations:

- ASI: Anthesis-silking interval.
- CWR: cell wall residue.
- BT: bundle tissues.
- DM: dry matter.
- DRT: dark rind tissues.
- ET: epidermis tissues.
- ETPP: estimated Penman evapotranspiration.
- Feest: esterified ferulic acid content.
- Feeth: etherified ferulic acid content.
- G subunit: guaiacyl lignin subunit
- H subunit: *p*-hydroxyphenyl lignin subunit
- LRT: light rind tissues.
- MGDD: modified growing degree days.
- MT: medullary tissues.
- NIRS: near infrared spectrometry.
- PAR: photosynthetic active radiation.
- PCest: esterified *p*-coumaric acid content.
- WW: well-watered condition in Mauguio.
- WD1: moderate water-deficit condition in Mauguio.
- WD: severe water-deficit condition in Mauguio.
- RW: rainfed condition in Versailles.
- S subunit: syringyl lignin subunit.
- SID: stress index.
- UFL: unité fourragère laitière (milk feed unit).

Introduction

Forage maize is the main component of the dairy cow feed ration in France (Carpentier and Cabon, 2011). While yield must be maintained to provide sufficient feed, forage maize is also evaluated through its milk-producing potential. In France, this potential is measured through the “barley feed unit” system, where one feed unit is equivalent to a kilogram of barley with an energetic potential of 1,760 kcal (Vermorel *et al*., 1987; INRA, 2018). The system was calibrated for a use in milk production *via* the “unité fourragère laitière” (milk feed unit, UFL) predictive equation (Andrieu, 1995; Peyrat *et al*., 2016). The resulting UFL value, expressed per 100 kg of organic matter, depends upon dry matter (DM) digestibility (in % of DM) with a very slight influence of protein content (MAT, in g/kg of organic matter). Due to an overall dependence upon DM digestibility (Baldy *et al*., 2017); combined with the low MAT variability in modern hybrids, UFL is often directly approximated to DM digestibility.

In optimal growing conditions, maize is split into two nearly equal fractions, the vegetative and the grain (Tolera *et al*., 1999; Arrigo and Stoll, 2012). The inclusion of the forage maize section in the official variety catalogue occurred in 1986 (Surault *et al*., 2005), but it wasn’t until 1998 that the UFL parameter was included as an official registration criterion (Perspectives Agricoles, n° 330). Analysis spanning from the 1950s and the 2000s revealed that while DM yield increased by 5 tons of DM/ha, there was a concurrent reduction in DM (2-point) and cell wall (CW) (5.5-point) digestibilities (Barrière *et al*., 2004). However, with the integration of UFL as an official registration criterion, this decrease was halted and UFL values stabilised from 2007 before rising again until 2015 (Surault *et al*., 2005; Baldy *et al*., 2017). Previous studies have highlighted the control of DM digestibility (and, therefore, UFL value) by CW content and digestibility, which are strongly correlated (Méchin et al., 2000 and 2005; Zhang et al., 2013; El Hage et al., 2018; Baldy *et al*., 2017).

Importantly, global-scale extreme climatic events' periodicity, intensity and duration have progressively increased over time, including in crop-growing regions (Cooper and Hammer, 1996; Hatfield and Dold, 2011; Chapman *et al*., 2012; Sen *et al*., 2017), with visible impacts on yield levels (Ray *et al*., 2015; Grassini *et al*., 2013). As most fields in France are located in humid regions, almost no forage maize surfaces are irrigated (Agreste, 2023), and are therefore particularly susceptible to drought events. Maize, as a summer plant, is sensitive to water stress, particularly during its flowering and subsequent grain-filling growth stages between July and August (Salter and Goode, 1967; Bänziger *et al*., 2000), as these periods require significant quantities of water (Elmore, 2012) to guarantee both pollination and correct grain yield (Denmead and Shaw, 1960; Reynolds and Langridge, 2016; Turc and Tardieu, 2018). Heat stress over these two growth stages can also exacerbate issues, jeopardizing pollen survival and seed setting and reducing potential grain yield (Schlenker and Roberts, 2009; Carter *et al*., 2016; Shao *et al*., 2021). The combination of both stresses is referred to as drought, and in France, have been found to reduce forage maize yield from 10 to 50% (Lemaire, 2008; Osborne and Wheeler, 2013; Iizumi and Ramankutty, 2016).

While this sensitivity to environmental extremes is well known, work on selecting maize for these conditions has remained firmly rooted in efforts for the grain

fraction. The result of past forage maize selection programs was based on higher grain yield (Lauer *et al*., 2001; Luque *et al*., 2006) or greater tolerance to higher plant density (Gonzalez *et al*., 2018). Furthermore, these higher yields may not only be due to selection efforts, with warmer climates playing a key role in yield increase (Taube *et al*., 2020). Comparable results are also found in water deficit conditions (Duvick *et al*., 2003; Campos *et al*., 2006; Cooper *et al*., 2014; Liu *et al*., 2023).

It is noteworthy that the maize CW is also affected by water deficit (El Hage et al., 2018 and 2021; Virlouvet et al., 2019). The CW is composed of structural elements such as polysaccharidic (cellulose and hemicelluloses) and phenolic compounds (lignin and *p*-hydroxycinnamic acids, *i.e*. esterified *p*-coumaric acid (PCest) and esterified and etherified ferulic acids (Feest and Feeth)) crucial for providing support against the plant environment (Carpita *et al*., 2001; Santiago *et al*., 2013). These components are primarily deposited before the flowering period (Jung, 2003; Jung and Casley, 2006; Zhang *et al*., 2019). Previous work has identified a decrease in the content of structural components during water deficit over this period, but also a change in lignin and other components distribution between rind and pith, benefitting CW digestibility in maize (Emerson *et al*., 2014; Hutiens, 2017; El Hage *et al*., 2018; Virlouvet et al., 2019; Ferreira, 2020). While the compositional study of this distribution is complex by biochemical quantifications, requiring a manual separation of rind and pith, histological alternatives can allow the rapid analysis of lignin distribution *via* FASGA (Fucsina, Alcian blue, Safranina, Glicerina and Aqua) stained cross-section images (Tolivia and Tolivia, 1987; Méchin *et al*., 2000; El Hage *et al*., 2018; El Hage et al., 2019). Therefore, the integration of qualitative traits alongside yield targets could provide essential breeding targets to improve overall forage quality, particularly to optimize water use efficiency under deficit conditions.

Here, we investigated the effects of eight different environmental conditions on a panel of 16 modern forage-maize hybrids representative of the French S0 (very early) and S1 (early) flowering earliness market. First, a comprehensive environmental stress index (SID) was established to precisely quantify the stress levels present under the different environmental conditions. Second, agronomic, biochemical and histological characterization were conducted to determine the impact of stress intensity on these different traits and globally survey the mechanism of regulation of maize forage digestibility.

2 - Materials and methods

2.1 - Stress management and field trials

Plants were grown at two environmentally contrasted INRAE experimental units (EU) in France across 2021 and 2022: Versailles-Saclay EU (Versailles, GPS: N: 48’48”33.391 / E: 2’5”7.237) and DiaScope EU (Mauguio, GPS: N: 43’36”52.438 / E: 3’58”34.419), hereafter referred to respectively as “Versailles” and “Mauguio”. Across both years, fields were sown with the same management practices aimed at reaching a density of 100,000 plants/ha, sown in an incomplete Latin square design wherein each variety is present in two rows under three blocks per condition. Slight differences

in planning did exist between both EUs, as in Versailles rows were 3 m long with a 0.8 m alley, while at Mauguio each row was 4.2 m long with a 0.8 m alley. A rainfed modality was repeated each year at Versailles (RW). For this modality, a drip-fed system was used to provide irrigation, when necessary, based on monitoring with a climatic station. Three different modalities were repeated each year at Mauguio with progressively decreasing levels of irrigation: a well-watered modality (WW) with a triweekly 20 mm irrigation dose; a moderate water-deficit modality (WD1) which received a 15 mm irrigation dose upon soil water tension reaching –125 kPa; and a severe water-deficit modality (WD) which received a 13 mm irrigation dose upon soil water tension reaching –300 kPa. These two stress modalities were applied from 25 days post-sowing, and all fields were separated by a 20 m border between modalities to avoid irrigation overlap. Stress levels were monitored at Mauguio using tools from the DiaPHEN platform: three pairs of two watermark tensiometers were present in each block per condition under a reference variety, at –30 and –60 cm, with the mean values used to trigger irrigation. These were installed alongside a pluviometer in each block. Slight differences affected both field trial years, leading to slight subtleties depending on the considered locations and conditions, as described below.

- **Versailles:** Annual differences significantly impacted growing conditions across both years in this location. In 2021, the Versailles field trial received nearly 360 mm of total rainfall across the growing period, but in 2022 this quantity decreased 52% to 171 mm. This decrease required an irrigation input of 232 mm in 2022, bringing total water input up to 403 mm, which was not required in 2021. Mean temperatures also increased across both years, increasing from 16.8 to 18.5 °C from 2021 to 2022 (**Table S1**).
- **Mauguio:** Rainfall did not significantly change across both years in Mauguio (113.5 mm in 2021, 116 mm in 2022), though the average temperature did increase from 22.2 to 23.8 °C from 2021 to 2022. In our two stressed conditions in 2021, irrigation was typically launched well before the tensiometer thresholds were reached as visual plant observations were more trusted. We forced ourselves to dictate irrigation on tensiometry data in 2022, resulting in a reduced total irrigation dose for the three irrigation modalities in 2022 (13.71% for WW, 17.78 for WD1, 4.99% for WD) (**Table S1**).

The different environmental conditions in both years, particularly in July during the flowering period in 2022, led us to consider the different modalities as separate conditions and to distinguish eight contrasted environmental conditions (*i.e.* RW 2021, WW 2021, WD1 2021 and WD 2021), and four in 2022 (RW 2022, WW 2022, WD1 2022, and WD 2022).

The hybrid material was selected from varieties experimented in the S0-S1 Post Registration Evaluation Network, a national collaboration between the French agricultural technical institute ARVALIS and the maize and sorghum section of the UFS (Varmaïs, 2024). The hybrids were selected during their final years in the evaluation network according to three criteria: (i) maximising the yield to UFL variability, (ii) accurately representing the current state of the S0/S1 forage maize market, and (iii) including diverse genetic and seed company diversity. Since varieties

remain in the network for a total of three years, some varieties could not be repeated in 2022. In 2021, 13 hybrids with a reduced flowering window were selected from eight different breeding companies. Eleven from this original panel were maintained for planting in 2022, along with five newly selected varieties, which had recently been included in the post-registration trial network (**Table S2**).

2.2 - Agronomic analysis and sample harvest

Throughout the plant growth cycle, measurements of key agronomic traits were noted in all locations and conditions. Flowering dates, both male (noted when at least 50% of the plants in a block had pollen pods that were at least two-thirds open) and female (noted when at least 50% of the plants in a block had visible silks), were recorded to determine the anthesis-silking interval (ASI). When the 32% DM harvest indicator was reached, four homogenous plants were harvested per block (two in each row) per variety per condition at the ground level. The total plant and ear insertion height alongside the fresh weight were then measured. After grinding the plants in a Viking GE 355, a representative sample of approximately 400 g was retained per block for drying in a forced-air oven at 55°C during 72h. The dried sample determined the block's %DM content, thereby allowing yield determination. It was then ground with a hammer mill (1 mm grid) for use in biochemical analysis. Additionally, for histological analysis, three internodes located just below the main ear were harvested for each variety in each block in all conditions and locations throughout both years and stored in 70% ethanol.

2.3 - Stress index and environmental analysis

The SID was developed iteratively, with the idea of retaining as few traits as possible while ensuring optimal accuracy in stress quantification, considering the effects of both water and heat stress as evenly as possible and on a daily basis. In this endeavour, the following equation is proposed:

$$\mathrm{SID} = \left(\left(\frac{soil\ water\ deficit\ (mm)}{easily\ accessible\ water\ reserve\ (mm)}\right) * 100\right) + \left(\frac{\left(\left(24 * \left(\frac{n°\ of\ hours\ spent > 30°C}{24}\right) + 1\right) * \left(\frac{maximum\ temperature\ of\ the\ day\ (°C)}{heat\ stress\ threshold\ (°C)}\right)\right)}{2400 + 1}\right)$$

This equation is made up of two main parts. The first, the water stress aspect, considers the percentage of utilisation of the available water reserve. This is usually calculated as a percentage, wherein if the percentages exceed 100%, the plants have theoretically used up all the available water and have entered a state of water stress. The value can be measured through different methods. Soil water tensiometers can be used, in conjunction with a known soil tension stress threshold, to measure a threshold overrun. In this paper, we calculated this part of the equation by dividing the soil water deficit by the easily accessible water reserve, both in mm, obtained using

the ARVALIS Irré-LIS® (irrelis.arvalisinstitutduvegetal.fr; Gendre *et al*., 2018; Gendre, 2020) irrigation decision-making tool (**Table S3**). The second heat aspect is a novel combination of traits to estimate the impact of heat stress on plant development. This aspect is split into two parts, the first aiming to quantify the duration of time spent above the specified heat stress threshold (30°C for maize), and the second considering the extent to which the maximum temperature reached during the day exceeded the heat stress threshold. This second adjustment attempted to account for the additional impact of higher overall temperatures reached during the day. The SID values were calculated according to the maize physiological phases. Two key stages were considered:

- 1st to 15th of July: this period covers both the male and female maize flowering periods. It was referred to as Period 1 (P1).
- 16th of May to 15th of August: this period covers the key physiological stages of maize development. It excluded stages more related to periods affecting the number of plants and desiccation stages and focused on the overall plant yield. This period was referred to as Period 2 (P2).

Additional environmental traits were acquired from weather stations installed at both experimental units, connected via the Climatik environmental INRAE database organised by the INRAE AgroClim unit. These included:

- The sum of the Total Water Input (TWI, combining both total rainfall and irrigation, when applicable, in mm) subtracted by the Penman Predicted Evapotranspiration (ETPP), abbreviated as TWI-ETPP and measured either as a daily mean or a sum for both periods across both years.
- The daily mean temperature (in °C) for both time periods.
- The mean daily air humidity (in %) for both time periods.
- The sum of the Photosynthetically Active Radiation, abbreviated to PAR (Joules per cm^2) for both time periods.
- The Heat Stress Duration, abbreviated to HSD (number of hours spent above 30°C) for both time periods.

SID values are positive in our method, as soil water deficit, as estimated by Irré-LIS, provides positive values. To analyse this type of data with the TWI-ETPP results, which are negative, the latter trait data were inverted when necessary.

2.4 - Biochemical analysis

Biochemical traits (**Table S4**) were measured through analysis conducted on distinct sample sets, each corresponding to a specific analysis. When reference is made to the number of blocks analysed in an experiment, this refers to the actual biological blocks sampled in the field. Unless otherwise specified, each experiment was performed with two technical repetitions. When referring to a sample, we therefore refer to an individual block from a variety within a given condition.

For DM samples, DM digestibility was measured for all varieties, blocks and conditions, totalling 195 samples in 2021 and 240 for 2022 using the method described in Lopez-Marnet *et al*., 2021. Digestible yield was then calculated on these samples (digestible yield = yield * (DM digestibility/100); Main *et al*., 2023). A 90-DM sample subset from the two studied years, limited to conditions from Mauguio was also assayed for soluble sugar content at the INRAE Lusignan site (39 in 2021, 48 in 2022). The *in vitro* digestibility of the non-starch and non-soluble carbohydrate plant fraction (IVDNSC), as described in Argillier *et al*., 1995, was calculated in this paper using a starch content predicted by an internal NIRS equation (IVDNSC = (100 * (DM digestibility – predicted starch content – soluble sugar content)) / (100 – predicted starch content - soluble sugar content)).

Following block-level analysis, using both agronomic and biochemistry data, to identify the presence of any block effects in the different locations and conditions, two representative blocks were retained per condition per year for CW residue (CWR) extraction (Effland, 1977), with 104 samples extracted in 2021 and 152 in 2022. CW digestibility was then measured for all extracted samples for both years (256 in total) using the same method as described for DM digestibility (Lopez-Marnet *et al*., 2021).

All CW samples (256 samples) were also assayed for lignin content by subjecting approximately 7 to 8 mg of extracted CW to an acetyl bromide treatment as presented in Fukushima and Hatfield, 2001, and dosed by spectrometry. Lignin structure and composition were also determined through thiacidolysis by treating 13 to 15mg of extracted CW with boron trifluoride and ethaniol heated at 100°C for 4h (oil bath), followed by lignin subunit and βO4 link dosing by gas chromatography (GC); Lapierre *et al*., 1986). Given the large number of samples and the throughput of the thioacidolysis assay, only one block per condition per year was assayed for thiacidolysis (52 in 2021, 64 in 2022). Results from thioacidolysis were expressed in subunit yields per the previously measured lignin content (µmol/g lignin content).

Additionally, 50 mg of CWR per sample (2 blocks for 2021, 104 samples; 1 block for 2022, 76 samples) was submitted to alkaline hydrolysis under NaOH 2N at ambient temperature for 20h to allow liberation of acids from ester links (Méchin *et al*., 2000) and alkaline hydrolysis under NaOH 4N at 170°C to allow liberation of both esterified and etherified acids. Following extraction (Culhaoglu *et al*., 2011), PCest, Feest and Feeth (measured by comparing quantities released between mild and severe alkaline treatments) were then analysed in high-performance liquid chromatography ultraviolet (HPLC-UV).

2.5 - Histological analysis

2.5.1 - Image acquisition and treatment

Histological analyses were carried out by combining the methods of Legland *et al*., 2017 and El Hage *et al*., 2021. Two of the three harvested internodes located below the ear previously stocked in 70% ethanol since the harvest were sampled at 1.5 cm under the upper node and cross-sections with thicknesses of 150 µm were obtained with a GSL1 sledge-microtome (Gärtner *et al*., 2014). These were then

stained under agitation as described by El Hage *et al.*, 2018, wherein internodes are stained for 24h in FASGA (1:8, v/v), washed for another 24h in distilled water, which is removed and replaced with clean water before mounting between slide and coverslip. The internodes were then mounted between the slide and coverslip, which were then sealed with hardening liquid. Images were then immediately acquired through an AxioImager Z2 Zeiss, as described in Legland *et al*., 2017. Cross-section images were obtained in a Metafer automated slide scanner platform (MetaSystems, GmbH, Altlussheim, Germany). Images were obtained with a 5x objective lens and then reduced in size *via* the MetaViewer software to obtain a final resolution of 5.17 µm per pixel.

2.5.2 - Image Segmentation data treatment and analysis

The resulting images were expertised to account for damage present on internodes due to both the microtome and the harvest condition. Image handling and modifications were performed using the ImageJ Fiji version (Schneider *et al*., 2012; Schindelin *et al*., 2012). If the internode cross-section damage was too important, requiring a correction of more than 5%, images were removed from the dataset. These represented no more than 30 samples out of an original 390 image set. Images were then automatically segmented utilising the ImageJ plugin developed by Lopez-Marnet *et al*., 2022. Briefly, this plugin, originally established for segmenting FASGA-stained maize internodes, segments 44 different tissues (alongside a few summary variables) in raw pixel amounts. The respective tissue pixel surface area is then divided by the total pixel size of the cross-section, allowing the calculation of each tissue type in a percentage of the total cross-section surface. The plugin quantifies different types of tissues depending on their localisation and colour. These include two types of rind tissues (Dark Rind Tissues, referred to as DRT; Light Rind Tissues, referred to as LRT), different medullary tissues (MT) in the pith, and several tissues linked either to the epidermis (ET) or to tissues close to or included within the vascular bundle (BT). The plugin also calculates sums of these tissues, alongside the total overall lignified and low lignified surfaces.

2.6 - Statistical analysis

Data was statistically analysed using R 4.3 with the RStudio interface (R Core Team, 2023; R Studio Team, 2023). Data was averaged across all blocks per variety for each condition per year. Data management and wrangling were performed using tidyverse and dplyr packages (Wickham *et al*., 2019 and 2023). Data normality was verified *via* Shapiro-Wilk testing and residual dispersion analysis. ANOVA analysis was performed utilising a linear model accounting for variety and condition effects. Additional analysis was also performed on the row and column field trial design effects for all conditions to identify any potential position effect within the field. If these effects were identified, they were included within the ANOVA model as covariables, otherwise the analysis was performed utilising a simpler model:

$$Y_{ijkl} = \mu + V_i + C_j + (VC)_{ij} + c_{jk} + r_1 + E_{ijkl}$$

Where Y_{ijkl} is the value for the given trait of the *i*th Variety in the *j*th Condition localized, if necessary if the *k*th column and the *l*th row within the field, with μ as the intercept. The decision to retain or not the additive model was calculated through an F test for interaction as described in Main *et al*., 2023. Due to the environmental analysis revealing the annual differences across both growth sites, we decided to analyse conditions on a year-per-year basis by combining the modality with the given year ("RW_2021", "RW_2022", etc).

Bar plots and dot plots were generated using the ggplot library (Wickham, 2016). When data points were sufficiently available, error bars were added by calculating the standard error values for each variable. Violin plots, with the attached internal data analysis, were generated by the ggstatsplot package (Patil, 2021). Principal component analysis (PCA) was performed using the factoextra package (Kassambara and Mundt, 2020), with analysis ran on the first fix dimensions and ellipse thresholds set to 95%.

Linear correlations were calculated using ggpbur (Kassambara, 2020). Pearson correlations with their associated p-values were calculated utilising the ggcor and corrplot packages (Kassambara, 2022; Wei and Simko, 2021). Linear multiple regression models were built utilising the olsrr package (Hebbali *et al*., 2023). In some model-generating runs, some variables may be added to the model without significantly increasing the model precision (R^2) or reducing the Root Mean Square Error (RMSE). To avoid these issues, and to therefore simplify the analysis, models were cut off when variable addition did not improve model precision by at least 4% or if not RMSE was not notably decreased.

Results

1. A stress index that considers the water deficit in the soil and the air temperature ranks the environmental conditions according to stress intensity

To investigate the effects of drought on maize forage quality, we grew a panel of modern forage maize hybrids over two years under four different water modalities representing a total of eight environmental conditions. To correctly identify annual differences and accurately quantify stress levels in the different environmental conditions, we created a comprehensive SID, considering soil and air (humidity and temperature) aspects.

For each environmental condition, we collected standard agroclimatic data across the two considered physiological phases (P1 and P2). A PCA was performed for all agroclimatic traits studied under the eight conditions. The first two dimensions of the PCA explained 93.9% of the variation of all agroclimatic traits (**Fig. 1A**). Dimension 1 explained 65.5% of the variation and obviously separated the year effect, with 2021 conditions being influenced by air humidity, while those in 2022 were influenced by temperature and PAR (**Table S5**). Interestingly, the year effect for 2022 appeared to

repeat the position of 2021 but pulled towards the right-hand side. Dimension 2 explained 28.4% of the variability and separated the stress intensities, with the WD conditions leading alongside plant water rain and irrigation minus ETPP (86.64%, **Table S5**). In contrast, the less stressed conditions appeared at the bottom of the graph. When considered as illustrative variables, the SID sums calculated over P1 and P2 were between water stress (rain & irrigation minus ETPP) and heat stress (Temperature, PAR) and tended to be closer to the water deficit traits. A significant negative correlation was also observed between SID values and plant yield (**Fig. 1B**) and height (**Fig. S1A**), and a significant positive correlation between SID values and ASI (**Fig. S1B**).

SID values were then averaged per half-month period from the 1st of June to the 15th of August across all conditions and both years, with these periods covering the most important physiological stages of maize, which also correspond to the times of greatest stress sensitivity. The decision to consider semi-monthly time windows instead of weekly periods was made to achieve sufficient periodic precision while avoiding analytical overload. The SID accurately quantified the condition differences for both water stress conditions (WD1 and WD) in 2021 and 2022, indicating a progressive increase in stress between the irrigated, moderate, and severe stress conditions during the male and female flowering periods (**Fig. 1C**). The two stress conditions gradually converged, as the growth stages transitioned to the grain-formation stages. While the SID values in the WW and RW conditions did not exceed the 100% thresholds, an annual effect was observed. The WW 2022 condition was visibly more stressed than the corresponding 2021 condition, but no significant index difference was noted for the two RW conditions in Versailles. Overall, these data showed that the SID correctly combined both hydric and thermic stress intensities and allowed the classification of our different conditions depending on their stress intensity levels. Linking these values to agronomic data allowed us to integrate the SID into our subsequent analysis.

2. Strong impact of stress intensity on yield, digestibility and *p*-hydroxycinnamic acid content

To accurately assess the effects of the different stress levels on agronomic and qualitative parameters, yield and DM digestibility were first measured from a set of 157 samples in 2021 (**Fig. 2A, Table I** and **Table S6**) and 241 samples in 2022 (**Fig. 2B, Table I** and **Table S6**). For both the humid RW and WW conditions, yields increased in 2022 compared to 2021, but these increases were not significant when the conditions were considered separately (**Table I**). With regards to DM digestibility over the two years, the digestibility values for the two WW conditions were also almost identical and did not differ statistically. In contrast, for the RW condition, a slight significant increase in DM digestibility could be observed in 2022 (**Table I**). For WD1, yield decreased significantly by 21.2% from 2021 to 2022 (**Table I**). The same significant decline was also noticed in the WD condition, with a 31.37% drop in yield in 2022. A notable divergence, however, occurs for DM digestibility, which was maintained over the two years for WD1, but decreased significantly for WD compared

to WD1 (**Table I**). This had clear consequences on digestible yields. While in 2021 some varieties under the WD1 condition were able to compensate for their reduced yields by increasing the DM digestibility, the reductions in 2022 were such that this compensation was unobtainable (**Table S6**). This was also noticeable at the mean level, with digestible yield remaining unchanged for the humid conditions yet falling by 22.6% for WD1 and by 36% for WD between 2021 and 2022. This decline was clearly visible at the variety level. Thus, in 2021, varieties J and E emerged for their resilience to stress conditions (variety J in WD 2021 was grouped with WD1 2021 individuals, while the same variety in WD1 2021 was grouped with those in WW 2021), or their overall performance under moderate stress (variety E yielded as much in WD1 2021 as in WW 2021) (**Fig. 2A**). Such distinctions were absent in 2022, with varieties firmly remaining inside their condition group (**Fig. 2B**).

It is noteworthy that soluble sugar content did not explain any variation, while a correlation between starch content and DM digestibility was found (**Fig. S2**). As stress intensity increased, the decrease in starch content was associated with the reduced production of ear (**Table I, Fig. 6**). Ears provide digestible starch, while stems and leaves contribute both soluble digestible fraction and non-soluble fraction consisting of CW traits and of non-total digestibility. DM digestibility is the result of the digestibility of these three compartments. As a result, the DM digestibility in WD1 increased due to both ear-provided starch and the increased CW digestibility. Despite a significant reduction in ear proportion, DM digestibility in WD was maintained at the same level as in WW (**Fig. 6**). This is especially evident when considering DM digestibility without variety B; **Table I**) due to the increase in CW digestibility. This prompted us to delve into CW-related traits. Lignin content showed small variations between hybrids within a given environment (**Table I**). The same trend was observed between environments, even under WD conditions (approximately a 1.5-point difference between WW and WD conditions in the same year, equating to a 10% variation; **Table I)**. On the other hand, *p*-hydroxycinnamic acid levels displayed a significant variability. The WD 2022 condition led to a 41% drop in PCest and a 19% drop in Feest (**Table I)**.

3. A combination of PCest and lignin content with pith and rind traits, enables partial separation of environmental conditions, particularly under stress

When combined across years and conditions, the ANOVA trait analysis revealed a wide range of significant interactions between conditions and variety for these traits (**Table S7**). Of the 57 traits presenting a significant interaction between condition and variety, the condition effect was greater than the variety effect in 89% of cases. The six traits for which the variety effect was greater, were those summing the total areas of lignified and non-lignified tissues and the four medullary-linked tissues. To assess the relationship between traits, PCA was also performed on individuals from all conditions, retaining all histological traits and all CW-related biochemical traits (*i.*e. CW digestibility, lignin content, structure and composition, and *p*-hydroxycinnamic acid content). The first two dimensions represented 27.6 and 13% of the global variance, respectively (**Fig. 2C**). While the first dimension was mainly characterised

by rind-related tissues (15 out of the top 20 traits, 52.39% of the dimension's variance, **Table S8**), the second dimension was characterised by the quantification of both blue and red-stained tissues (top 2 traits, 21.9% of dimension variance, **Table S8**), quickly followed by medullary tissues (13 out of the top 20 traits, 65.07% of dimension variance). Furthermore, in the first dimension, the top 20 variables were dominated by traits where the effect of condition outweighed that of the variety, while varietal effects only began to take a dominant position in the second dimension (**Table S8**). These two dimensions did not visually separate any of the condition-related ellipses. The inclusion of the third dimension, which accounted for 11.2% of the total variance and was characterised by a combination of biochemical traits, particularly lignin and PCest content (21% of the variance) and histology traits linked both to the rind (16.19%) and pith (21.71%)**,** enable partial condition separation, particularly for stressed conditions (**Fig. 2D**). This separation was dependent on stress intensity, clearly explained by the illustrative SID trait consistent with dimension three. The SID trait was opposite to yield, enabling a grouping of the environmental conditions into three distinct groups: (i) a "humid group" composed of WW and RW conditions for 2021 and 2022, (ii) a "moderate to severe-stress group" composed of WD 2021, WD1 2021, and WD1 2022, and finally (iii) a "severe stress" group with WD 2022. In this configuration, a year separation was achieved around the origin of the first dimension, separating 2022 data to the left and 2021 data to the right.

4. Histological tissues play different roles in relation to both CW digestibility and composition

To understand the distinct roles played by biochemical traits and lignin repartition, and identify those affected by stress intensity, we then analysed changes in key tissues, such as the quantifications of both blue and red-stained tissues, known to be impacted by water stress in our segmentation results. Agronomic and DM-related biochemical traits were added as active traits to identify any potential relationships between histological or CW-related traits and overall yield and digestibility. Overall correlations were then calculated per condition. We identified that the number of significant correlations between the three main types of histological traits (*i.e.* rind DRT and LRT tissues and medullary tissues) and biochemical traits found in the CW (lignin content, structure and composition) were affected by the different growing conditions (**Fig. S3**). In humid conditions, most correlations between biochemical traits were found to be for the DRT traits. As the level of stress intensity increased, the number of correlations between biochemical traits and DRT progressively decreased and were replaced with correlations to LRT (and medullary tissues to a lesser extent). There was no visible change in the area of the rind occupied by DRT (**Fig. S4A**) or LRT (**Fig. S4B**) until 2022. It was tempting to explain this year difference by lignin content, but there seemed to be no year effect for this trait, although a greater reduction in the WD 2022 condition could be noted (**Table I**). This difference between tissues was also noticeable when visually observing the output of the image segmentation plugin on variety H, our agronomic reference, across the 4 conditions of 2022 (**Fig. 3A** to **Fig. 3D**). In the rind, LRT area progressively decreased under stress conditions, inversely to the area of DRT. The opposite was observed under humid conditions. Effects were

also observed in the pith. As stress levels increased, a blue low-lignified band progressively increased under the rind section. Under humid conditions, this band was decreased and intercepted before the rind by a layer of lignified tissues. Taken together, five main tissues were responsible for a large part of the previously observed PCA variation: lignified and low lignified tissues, DRT, LRT, and medullary tissues (**Fig. S5** to **Fig. S12** and **Table S8**). We found that DRT traits were negatively correlated with CW digestibility, while LRT traits were positively correlated (**Table S9**). This may be explained by the cell wall composition, as we found that DRT was often positively related to lignin content, β04 yield, S subunit content, PCest content, Feest content, and %S-PC, which were in turn negatively correlated with CW digestibility (**Table S9**). Conversely, LRT was often negatively correlated with some of the same traits with which DRT was positively correlated (lignin content, S subunit content, PCest, and Feest). Interestingly, in the WD1 and WD 2022 conditions, LRT traits were positively correlated with lignin structures such as PCest and β04 yield, while in these conditions, DRT was not significantly related to these biochemical traits. Analysis for medullary tissues was complex, as the different tissues can represent both highly and lowly lignified pith tissues. Thus, we did find correlations between these histological pith traits and biochemistry (**Table S9**), but they were a mix of negative and positive correlations depending upon the trait and the condition.

To deepen the correlations between the various traits, we examined their relationships using network plotting. Under humid conditions, represented by RW 2021, the traits were divided into two distinct modules, where module 1 consisted mainly of medullary tissues and sums of lignified tissues, while module 2 was a combination of rind tissues that outnumbers biochemical and agronomic traits **(Fig. 4A** and **Fig. S13).** In the case of moderate stress, represented by WD1 2021, the traits were divided into three groups **(Fig. 4B** and **Fig. S13**). Module 1 consisted mainly of medullary and lignified tissues, while module 2 contained histological rind traits. The third module was a combination of biochemical and histological traits from the rind and pith. It was labelled “biochemistry” because most of the traits in this module were biochemical in nature. This type of separation continued under the severe stress conditions (**Fig. 4C**). In WD 2022, module 1 also contained mainly medullary traits, while module 2 was dominated by rind. Again, the third module consisted of a mixture of biochemical traits and rind and pith traits. Interestingly, in both stress groups, the third module containing biochemistry traits was linked to histological traits in the other modules via rind tissues (DRT7 for WD1 2021; LRT7 for WD 2022).

5. Histological traits contribute progressively more to CW digestibility under moderate stress conditions than under humid conditions

To determine the factors responsible for CW digestibility variation under stress scenarios, stepwise multiple linear regression models were run per condition and year (**Fig. 5**). The models were examined both at the combined level and at the individual year level to determine the annual effects. The various predictors present in each model were listed in the order of their inclusion in the model, as well as the percentage of variation explained by their inclusion. When looking at all years combined, 57% of

CW digestibility was explained by associations with four biochemical traits (lignin content, 32%; structure, 14%; *p*-hydroxycinnamic acids, 11%). These predictors changed depending on the year considered. In 2021, CW digestibility was explained to 77% by associations with three biochemical traits (lignin content; 57%; structure, 11%; *p*-hydroxycinnamic acids 9%), and to 6% by a link to one pith histological trait. The 2022 model was more similar to that of the combined years. CW digestibility was explained to 47% by four biochemistry traits (lignin content, 19%; structure, 19%; *p*-hydroxycinnamic acids, 9%).

When considering the humid conditions, we found that 86% of the CW digestibility variation was explained in RW 2021, of which 64% was due to two biochemical traits (*p*-hydroxycinnamic acids, 47%; lignin structure, 17%) and 22% was due to two histological traits (pith traits, 22%). In RW 2022, however, CW digestibility was only explained by one histological pith trait, with an R^2 of 7%. In WW 2021, 92% of CW digestibility was explained by two lignin composition traits. In WW 2022, the model explained 84% of CW digestibility, of which 78% was explained by three biochemical traits (lignin content, 44%; *p*-hydroxycinnamic acids, 34%), and 6% by one histological pith trait.

For moderate stress conditions, CW digestibility was found to be explained up to 89%, with the importance of biochemical traits decreasing with stress intensity (from 57% to 38%), while the importance of histological traits increased (from 24% to 52%). It is noteworthy that under moderate stress conditions (WD1 2021), lignin content mainly explained CW digestibility, while under more stress conditions (WD 2021 and WD1 2022), *p*-hydroxycinnamic acids contributed more to the explanation of CW digestibility. Furthermore, rind traits were found to contribute more than pith traits under moderate stress condition (24% *vs* 7%) than under more stress conditions (12% *vs* 24%). Surprisingly, under severe stress conditions (WD 2022), it was found that 78% of CW digestibility could be explained by three biochemical traits (*p*-hydroxycinnamic acids, 65%; lignin content, 13%), and only 7% by one histological pith trait.

Discussion

1. The simple but robust stress index provides a key environmental ranking tool

As climate change progresses, extreme climatic events, including droughts, are expected to increase over the next decade (Spinoni *et al*., 2017). These are likely to combine the effects of water stress with increased overall heat, which should further impair agronomic performance (Moore *et al*., 2021). Limited water supplies (Molden, 2013) mean that the agricultural sector's response to these overall drier conditions will require some form of irrigation management to optimise overall water use. Calculating a plant's water requirements is intricate, as they depend on the species, soil type, and stage of the growth cycle (Mirhashemi and Panahi, 2021). To track and quantify the combined impact of water and heat stress, we developed the comprehensive and robust SID that can be rapidly determined at different plant development stages. In

contrast to the SID, traditional stress evaluation indexes such as the Crop Water Stress Index (Idso *et al*., 1981; Jackson *et al*., 1981) require manual and complex measurements, while more modern equivalents tend to focus mainly on water stress levels only (Hernández-López *et al*., 2024). The successful application of the SID under the eight environmental conditions we compared, which provided a key ranking of the conditions, along with the observed impact of heat stress in 2022, underscores the importance of considering both soil and air stress aspects. Additionally, the SID was designed to incorporate as few traits as possible and was constructed using traits that can be obtained relatively easily from meteorological or irrigation tools.

While obtaining the SID is straightforward, its accuracy could be improved by integrating measured soil water deficit through tensiometry data. Furthermore, canopy temperature sensors would greatly improve our results, as our current SID does not account for the effects of canopy cover and shading, though this will require further development. Despite not currently included in irrigation decision support, integrating the SID into existing tools would be feasible. Most commercially available tools already require access to a nearby Météo France or personal agricultural weather station, which routinely measure the data required to calculate the SID. Integrating the SID into such a tool would permit irrigating farmers to more accurately control when to irrigate plants based on their stress level.

In the literature, it is widely recognized that DM and CW digestibilities in grasses increase with the water deficit (Emerson *et al*., 2014; dos Santos *et al*., 2015; El Hage *et al*., 2018; Néné-bi *et al*., 2022; Main *et al*., 2023). However, the results of the severe stress experienced in 2022 indicate that we have reached a new response threshold for DM digestibility under the combined effect of severe water and heat stress. This led to a significant decrease in DM digestibility compared to the moderate stress conditions, while maintaining a level comparable to humid conditions. Interestingly, for some varieties (G, H, M and R), the DM digestibility did not decrease significantly between WD and WD1 2022, suggesting that variety-condition interactions still occur even under severe stress conditions. These findings suggest that genetic improvement remains feasible under these challenging growth conditions.

2. Under severe stress, *p*-hydroxycinnamic acids absorb the majority of the decrease in phenolic compounds synthesis, while lignin levels remain stable

Several studies across various species have demonstrated that water stress leads to a decrease in lignin content (Moura et al., 2010; Dos Santos et al., 2015; Van Der Weijde et al., 2017; Perrier et al., 2017; EL Hage et al., 2018), as well as in PCest when investigated (El Hage et al., 2018). Furthermore, although studies focusing on the isolated effect of heat stress are rarer, they suggest an influence of heat on the lignification process (Bala *et al*., 2016). The synthesis of phenolic compounds represents a significant and irreversible investment of carbon and energy for the plant, subject to various regulatory levels. It is believed that there is a decrease in the allocation of carbon to phenolic compounds in favour of synthesizing soluble

compounds, which may participate in osmoregulation and storage to facilitate recovery when water stress stops (Perrier et al., 2017). It is also commonly asserted that the lignin synthesized under stress have modified structure and composition. Cesarino (2019) points out the highly variable response to biotic and abiotic stresses, indicating that no definitive conclusions can be drawn regarding the specific role of individual lignin monomers in response to stress. Our study revealed that irrespective of the stress intensity, the composition and structure of the lignin remained unchanged. Furthermore, we demonstrated that through the selection for digestibility, breeders indirectly stabilized lignin content, which is strongly constrained in terms of both inter-genotypic variations and inter-environmental variations. Lignin plays an important structural role in protecting plants against pest attacks, maintaining overall plant health, and providing support to vascular tissues, particularly to withstand turgor pressure (Shu *et al*., 2021). Consequently, the increasing stresses impose an energetic and carbon economy on maize hybrids, primarily impacting the synthesis of PCest, and secondarily affecting Feest and Feeth. Ferulic and *p*-coumaric acids serve as intermediates in the lignin biosynthetic pathway (Peracchi *et al*., 2024). The regulation put in place in maize hybrids under varying degrees of water and heat stress is therefore quite remarkable in terms of ensuring that lignin content is maintained and that the drop in C flux is passed on to *p*-hydroxycinnamic acids.

3. The impact of biochemical and histological traits on CW digestibility varies depending on the stress intensity

To identify potential alternatives to lignin content in enhancing CW digestibility, we used an integrative multitrait approach, combining agronomic, biochemical and histological data across contrasted environments. Our findings under humid conditions underscored the significance of *p*-coumaroylation and lignin structure, consistent with previous works (Méchin et al., 2001 and 2005; Riboulet *et al*., 2008; Zhang et al., 2011). However, biochemical traits may have overshadowed histological traits, as they showed a significant impact on variability and could predict a small portion of CW digestibility under specific environmental conditions. As stress levels increased, histology played a more significantly role, with lignin distribution becoming as influential as lignin content, *p*-coumaroylation and lignin composition (**Fig. 5**). Under severe stress conditions, the role of lignin distribution returned to the level found under humid conditions, while lignin *p*-coumaroylation and content regained importance. This shift coincided with the maintenance of DM digestibility under severe stress compared to WW conditions (**Fig. 6**), attributed to the maintenance of CW digestibility. Intriguingly, variety B, which had the lowest DM digestibility under the severe stress condition, also displayed the lowest starch content. We hypothesise that the reduction in grain yield in variety B overrides the typical response of digestibility to stress intensity when surpassing the threshold of severe stress. As future environmental conditions are likely to be a combination of moderate to severe stress, it is essential to further investigate the impact of these combined stress conditions on future forage quality research. Such studies will need to combine both biochemical and histological approaches, as we found a significant non-redundancy of both types of traits

depending on the environment considered. The delayed response of histological traits to stress levels is consistent with previous findings indicating that biochemical traits in maize (El Hage *et al*., 2018; Virlouvet *et al*., 2019; Main *et al*., 2023) and other grasses (Luquet *et al*., 2019; Van Der Weijde *et al*., 2017) exhibit earlier response to lower stress levels, in contrast to histology which tends to respond only under pronounced stress intensities (El Hage, 2018; El Hage *et al*., 2021).

The different histological tissue types associated to CW digestibility variations were also affected by stress intensity, with DRT and LRT showing differential responses under the 2022 environmental conditions. The combined stresses during that year likely unveiled histological disparities, as previously mentioned. Changes in composition between DRT and LRT, and not only between the overall rind and pith, could also explain the variations observed in 2022. Under the humid conditions of this year, DRT was positively correlated with PCest and β04 yield, while LRT was negatively correlated. This order of correlation changes in WD1 2022 and WD 2022, with LRT now being positively associated with these highly indigestible CW elements. With increasing load intensity, denser elements would preferentially deposit in the LRT, closer to the pith, than in the DRT, which is closer to the epidermis. Since the LRT-to-rind ratio was much smaller than the DRT ratio under WD 2022, a highly indigestible LRT ring would form under severe stress conditions, which would be denser than those found at other stress levels. Plants grown under severe stress conditions also exhibited a blue ring, a phenomenon previously observed only in inbred maize lines (Zhang et al., 2013; El Hage et al., 2018; Zhang et al., 2019). While we had previously identified such bands, albeit to a lesser extent, in hybrids, the WD 2022 plants are the first commercial hybrids in our studies to replicate these results from inbred lines. This blue ring is reduced under humid conditions, but the use of the new FASGA image segmentation plugin (Lopez-Marnet et al., 2022) has further permitted the identification of a smaller red ring in these conditions. This red ring appears adjacent to the space between the nonlignified cortical parenchyma cells and the rind, progressively becoming more prominent under humid conditions. This thin layer of lignified cells is not actually present in the rind and appears to be a form of parenchyma. It is conceivable that under these conditions, the plant's overall height and the ear's weight (located just above this internode) promote a lignification pattern with a secondary layer of densely lignified tissues in the pith just before the rind. This could act as an internal structural support layer to assist the rind. Given that the rind is a denser tissue that is more prone to breakage, this more malleable dense-pith ring could serve as a more elastic support link. Its absence in the individuals of WD 2022 (and in all conditions in 2021) could be explained by this greater amount of denser DRT.

Conclusion

Through precise control of different water stress conditions and assessment via the SID, we gained insights into the impact of increased stress levels on both the yield and quality of forage maize (**Fig. 6**). Our study underscores the importance of prioritizing enhancements in CW digestibility under stress conditions to maintain or

enhance DM digestibility, thus affecting the energy content of forage maize. Our findings also revealed the regulatory mechanisms at play in maize hybrids under severe water and heat stress, ensuring the maintenance of lignin content, while channelling the decrease in carbon flux toward *p*-hydroxycinnamic acids. Finally, our study unveils that moderate water and heat stress serve as an ideal environmental condition for improving digestible yield, with both biochemical and histological traits exerting similar influence.

Table I. Impact of the environmental conditions on the main agronomic and biochemical traits studied. Mean values are indicated. Different letters for the same trait correspond to statistically significant differences between conditions (*P*<0.05). na: not appropriate.

Traits	RW 2021	RW 2022	WW 2021	WW 2022	WD1 2021	WD1 2022	WD 2021	WD 2022
Yield (ton DM/ha)	16.69^{b}	17.42^{ab}	17.36^{ab}	18.06^{a}	14.29^{c}	11.26^{d}	10.20^{d}	7.00^{e}
Whole ear proportion in yield (%)	*na*	40.59^{a}	*na*	34.47^{b}	*na*	30.33^{c}	*na*	19.62^{d}
DM digestigility (%DM)	67.35^{d}	69.15^{bc}	69.5^{bc}	70.26^{b}	73.68^{a}	72.63^{a}	73.33^{a}	68.38^{cd}
DM digestigility without variety B (%DM)	67.36^{c}	69.26^{b}	69.4^{b}	70.28^{b}	73.58^{a}	72.65^{a}	73.42^{a}	68.8^{bd}
Cell Wall content (%DM)	49.88^{b}	47.63^{bc}	45.87^{c}	44.11^{de}	42.57^{e}	44.32^{de}	44.65^{de}	52.87^{a}
CW digestibility (%CWR)	32.96^{de}	34.02^{cd}	30.94^{e}	34.22^{bcd}	35.25^{abc}	37.04^{a}	36.25^{ab}	36.69^{a}
Lignin content (%CWR)	15.78^{ab}	15.39^{bc}	15.93^{a}	15.77^{ab}	15.12^{cd}	14.86^{d}	14.72^{d}	14.11^{e}
PCest (mg/g CWR)	15.84^{a}	13.28^{bc}	15.03^{a}	15.88^{a}	13.42^{b}	11.89^{cd}	11.35^{d}	9.41^{e}
Feest (mg/g CWR)	8.52^{a}	7.62^{bc}	7.72^{bc}	6.9^{c}	8.01^{ab}	7.5^{bc}	7.42^{bc}	5.62^{d}
Feeth (mg/g CWR)	2.88^{a}	3.08^{a}	2.02^{bc}	2.6^{ab}	2.63^{ab}	2.74^{ab}	1.72^{c}	2.67^{ab}
Fetot (mg/g CWR)	11.28^{a}	10.64^{ab}	9.74^{cd}	9.51^{cd}	10.63^{ab}	10.25^{bc}	9.14^{de}	8.29^{e}
H subunit (µmol/g lignin content)	14.2^{a}	14.38^{a}	15.05^{a}	13.09^{a}	15.18^{a}	13.65^{a}	14.9^{a}	15.52^{a}
G subunit (µmol/g lignin content)	333.13^{a}	326.41^{a}	351.24^{a}	320.53^{a}	344.11	307.66^{a}	320.3^{a}	331.82^{a}
S subunit (µmol/g lignin content)	317.67^{a}	326.97^{a}	339.8 ^{a}	353.23^{a}	343.18^{a}	325.38^{a}	325.63^{a}	336^{a}

Supplementary data list

Table S1: Main climatic and maintenance data related to the eight different conditions studied.

Table S2: Varieties used in various growing conditions at Mauguio and Versailles during 2021 and 2022.

Table S3: Water balance status and overall environmental data included in the SID equations throughout the different studied conditions.

Table S4: Biochemical traits used in the article, along with their corresponding laboratory-measured units.

Table S5: Dimension contribution and composition for the environmental PCA analysis.

Table S6: Main trait variability within the studied datasets.

Table S7: ANOVA analysis for all traits studied across conditions is provided, along with the model and significance levels.

Table S8: Top 20 contributors to the first three dimensions in the the PCA analysis.

Table S9: Pearson correlations between studied traits.

Fig. S1: Verifying SID biological compatibility through correlations to agronomic traits.

Fig. S2: Studying overall impact of agronomic traits on DM digestibility.

Fig. S3: Quantifying significant correlations between histological and biochemical traits.

Fig. S4: Quantifying LRT-to-rind ratio under the different environmental conditions.

Fig. S5: Correlations between the different traits for RW 2021.

Fig. S6: Correlations between the different traits for RW 2022.*Fig. S7*: Correlations between the different traits for WW 2021.

Fig. S8: Correlations between the different traits for WW 2022.

Fig. S9: Correlations between the different traits for WD1 2021.

Fig. S10: Correlations between the different traits for WD1 2022.

Fig. S11: Correlations between the different traits for WD 2021.

Fig. S12: Correlations between the different traits for WD 2022.

Fig. S13: Network plots between the investigated traits under the different environmental conditions for agronomic, biochemical and histological traits.

Author contribution:

SC, VM, AU and NM designed the study. The field trials were organised by SC, VM, together with MR and OM for Versailles, and by FM and SR for Mauguio. Monitoring experiments and irrigation and field observations were conducted by FM, SF and SR for Mauguio. MPJ was responsible for both harvesting and laboratory coordination. OM, MPJ, CD, MR, PLLM, ALM, FM, VM and SC collected the samples. DM digestibility was performed by OM and SG. CWR extraction and CW digestibility were obtained by MPJ, SG and OM. Nitrogen content was measured by SG and AM. Soluble sugar content was measured by CB and GR. Lignin content was measured by OM and MPJ. Thioacidolysis was performed by MPJ and OM. Alkaline hydrolysis was performed by SG and VM. Internode slides were obtained by SG and OM. Slide staining and microscope acquisition were performed by OM, SG, MR, ALM, VM, SC and MPJ. Image extraction, analysis and correction were performed by OM, PLLM and SG. Data integration and analysis were done primarily by OM with assistance from ALM, then by VM and SC. OM, VM, and SC wrote the manuscript. All authors read and approved the submitted manuscript.

Funding:

This work is supported by the Plant2Pro Carnot institute in the frame of the MAMMA MIA project. Plant2Pro is supported by ANR (agreement #20 CARN 0024 01). This work has benefited from the support of the IJPB's Plant Observatory platform PO-Cyto. The IJPB laboratory also benefits from the support of the Saclay Plant Sciences-SPS (ANR-17-EUR-0007).

Data availability statement:

All raw data supporting the conclusions of this article is available, upon contact with the authors and without undue reservation.

Acknowledgments:

We sincerely acknowledge the UE teams from DiaScope (Mauguio, France) and Versailles-Saclay (Versailles, France) for their precise and rigorous work on the different field trials. We also wish to thank the INRAE Lusignan URP3F team for their fast reactivity and precise dosing of the soluble sugar content, the INRAE Versailles APSYNTH team for their assistance with the alkaline hydrolysis and thioacidolysis experiments, Dominique Kermarrec from the INRAE Ploudaniel for sample grinding, and the IJPB Plant Observatory Cytology/Imagingplatform. We finish by thanking all members of the "Biomass Quality and Interactions with Drought" team past and present, and members of the different ARVALIS teams implicated in the project.

Conflict of interest:

All authors declare that the research was conducted in the absence of any commercial or financial relationships that could be construed as a potential conflict of interest.

References:

AGRESTE. 2023. *Statistique agricole annuelle 2022 - Chiffres provisoires*.

Andrieu J. 1995. Prévision de la digestibilité et de la valeur énergétique du maïs fourrage à l'état frais. INRAE Productions Animales **8**, 273–274.

Argillier O, Barrière Y, Hébert Y. 1995. Genetic variation and selection criterion for digestibility traits of forage maize. Euphytica **82**, 175–184.

Arrigo Y, Stoll P. 2012. Estimation de la valeur nutritive de l'ensilage de maïs.

ARVALIS. 2024. *Varmäis*.

Bala S, Asthir B, Bains NS. 2016. Syringaldazine peroxidase stimulates lignification by enhancing polyamine catabolism in wheat during heat and drought stress. Cereal Research Communications Cereal Research Communications **44**, 561–571.

Baldy A, Jacquemot M-P, Griveau Y, Bauland C, Reymond M, Mechin V. 2017. Energy Values of Registered Corn Forage Hybrids in France over the Last 20 Years Rose in a Context of Maintained Yield Increase. American Journal of Plant Sciences **08**, 1449–1461.

Bänziger M, Edmeades GO, Beck DL, Bellon MR. 2000. Breeding for drought and nitrogen stress tolerance in maize: From theory to practice.

Barrière Y, Emile JC, Traineau R, Surault F, Briand M, Gallais A. 2004. Genetic variation for organic matter and cell wall digestibility in silage maize. Lessons from a 34-year long experiment with sheep in digestibility crates. Maydica **49**, 115–126.

Campos H, Cooper M, Edmeades G, Löffler C, Schussler J, Ibañez M. 2006. Changes in drought tolerance in maize associated with fifty years of breeding for yield in the US Corn Belt. Maydica **51**, 369–381.

Carpentier B, Cabon G. 2011. Le maïs fourrage : élaboration du rendement et de la qualité, récolte et conservation. 13.

Carpita NC, Defernez M, Findlay K, Wells B, Shoue DA, Catchpole G, Wilson RH, McCann MC. 2001. Cell Wall Architecture of the Elongating Maize Coleoptile. Plant Physiology **127**, 551–565.

Carter EK, Melkonian J, Riha SJ, Shaw SB. 2016. Separating heat stress from moisture stress: analyzing yield response to high temperature in irrigated maize. Environmental Research Letters **11**, 094012.

Cesarino I. 2019. Structural features and regulation of lignin deposited upon biotic and abiotic stresses. Current Opinion in Biotechnology **56**, 209–214.

Chapman SC, Chakraborty S, Dreccer MF, Howden SM. 2012. Plant adaptation to climate change—opportunities and priorities in breeding. Crop and Pasture Science **63**, 251–268.

Cooper M, Gho C, Leafgren R, Tang T, Messina C. 2014. Breeding drought-tolerant maize hybrids for the US corn-belt: discovery to product. Journal of Experimental Botany **65**, 6191–6204.

Cooper M, Hammer GL, C.A.B. International, International Rice Research Institute, International Crops Research Institute for the Semi-arid Tropics (Eds.). 1996. *Plant adaptation and crop improvement*. Wallingford, Oxon, UK: CAB International in association with the International Rice Institute and the International Crops Research Institute for the Semi-arid Crops.

Culhaoglu T, Zheng D, Méchin V, Baumberger S. 2011. Adaptation of the Carrez procedure for the purification of ferulic and p-coumaric acids released from lignocellulosic biomass prior to LC/MS analysis. Journal of Chromatography. B, Analytical Technologies in the Biomedical and Life Sciences **879**, 3017–3022.

Denmead OT, Shaw RH. 1960. The Effects of Soil Moisture Stress at Different Stages of Growth on the Development and Yield of Corn1. Agronomy Journal **52**, 272–274.

Duvick DN, Smith JSC, Cooper M. 2003. Long-Term Selection in a Commercial Hybrid Maize Breeding Program. Plant Breeding Reviews. John Wiley & Sons, Ltd, 109–151.

Effland MJ. 1977. Modified procedure to determine acid-insoluble lignin in wood and pulp. Tappi;(United States) **60**.

El Hage F, Legland D, Borrega N, Jacquemot M-P, Griveau Y, Coursol S, Méchin V, Reymond M. 2018. Tissue Lignification, Cell Wall p-Coumaroylation and Degradability of Maize Stems Depend on Water Status. Journal of Agricultural and Food Chemistry **66**, 4800–4808.

Elmore R. 2012. Stress, anthesis - silk interval and corn yield potential. https://crops.extension.iastate.edu/cropnews/2012/07/stress-anthesis-silk-interval-and-corn-yield-potential.

Emerson R, Hoover A, Ray A, *et al.* 2014. Drought effects on composition and yield for corn stover, mixed grasses, and *Miscanthus* as bioenergy feedstocks. Biofuels **5**, 275–291.

Gärtner H, Lucchinetti S, Schweingruber FH. 2014. New perspectives for wood anatomical analysis in dendrosciences: The GSL1-microtome. Dendrochronologia **32**, 47–51.

Gendre S. 2020. Focus - Irré-LIS®, exemple d'outil d'aide à la décision en irrigation. Sciences Eaux & Territoires, 72–75.

Gendre S, Descazeaux P, Soenen B, Bouthier A. Development of an irrigation water requirements model on grain maize.

Gonzalez VH, Tollenaar M, Bowman A, Good B, Lee EA. 2018. Maize Yield Potential and Density Tolerance. Crop Science **58**, 472–485.

Gonzalo F. 2020. Does drought stress improve fiber digestibility? Hay & Forage grower.

Grassini P, Eskridge KM, Cassman KG. 2013. Distinguishing between yield advances and yield plateaus in historical crop production trends. Nature Communications **4**, 2918.

Hatfield JL, Boote KJ, Kimball BA, Ziska LH, Izaurralde RC, Ort D, Thomson AM, Wolfe D. 2011. Climate Impacts on Agriculture: Implications for Crop Production. Agronomy Journal **103**, 351–370.

Hebbali A. *olsrr: Tools for Building OLS Regression Models.*

Hernández-López JA, Andrade HJ, Barrios M. 2024. Agricultural drought assessment in dry zones of Tolima, Colombia, using an approach based on water balance and vegetation water stress. The Science of the Total Environment **921**, 171144.

Hutjens MF. 2017. How environment affects forage digestibility. AG Proud **Progressive dairy**.

Idso SB, Jackson RD, Pinter PJ, Reginato RJ, Hatfield JL. 1981. Normalizing the stress-degree-day parameter for environmental variability. Agricultural Meteorology **24**, 45–55.

Iizumi T, Ramankutty N. 2016. Changes in yield variability of major crops for 1981–2010 explained by climate change. Environmental Research Letters **11**, 034003.

Jackson RD, Idso SB, Reginato RJ, Pinter Jr. PJ. 1981. Canopy temperature as a crop water stress indicator. Water Resources Research **17**, 1133–1138.

Jung H-JG. 2003. Maize stem tissues: ferulate deposition in developing internode cell walls. Phytochemistry **63**, 543–549.

Jung HG, Casler MD. 2006. Maize Stem Tissues: Cell Wall Concentration and Composition during Development. Crop Science **46**, 1793–1800.

Kassambara A. 2022. ggcorrplot: Visualization of a Correlation Matrix ussing ‘ggplot2’. R package version 0.1.4, https://CRAN.R-project.org/package=ggcorrplot>. *in press*.

Kassambara A. 2023. *ggpubr: ‘ggplot2’ Based Publication Ready Plots.*

Kassambara A, Mundt F. 2020. Extract and Visualize the Results of Multivariate Data Analyses [R package factoextra version 1.0.7].

Lapierre C, Monties B, Rolando C. 1986. Preparative Thioacidolysis of Spruce Lignin: Isolation and Identification of Main Monomeric Products. Holzforschung **40**, 47–50.

Lauer JG, Coors JG, Flannery PJ. 2001. Forage Yield and Quality of Corn Cultivars Developed in Different Eras. Crop Science **41**, 1449–1455.

Legland D, El-Hage F, Méchin V, Reymond M. 2017. Histological quantification of maize stem sections from FASGA-stained images. Plant Methods **13**, 84.

Lemaire G. 2008. Sécheresse et production fourragère. Innovations Agronomiques **2**, 107.

Liu Y, Hou P, Zhang W, Xing J, Lv T, Zhang C, Wang R, Zhao J. 2023. Drought resistance of nine maize cultivars released from the 1970s through the 2010s in China. Field Crops Research **302**, 109065.

Lopez-Marnet P-L, Guillaume S, Jacquemot M-P, Reymond M, Méchin V. 2021. High throughput accurate method for estimating in vitro dry matter digestibility of maize silage. Plant Methods **17**, 89.

Lopez-Marnet P-L, Guillaume S, Méchin V, Reymond M. 2022. A robust and efficient automatic method to segment maize FASGA stained stem cross section images to accurately quantify histological profile. Plant Methods **18**, 125.

Luque SF, Cirilo AG, Otegui ME. 2006. Genetic gains in grain yield and related physiological attributes in Argentine maize hybrids. Field Crops Research **95**, 383–397.

Luquet D, Perrier L, Clément-Vidal A, *et al.* 2019. Genotypic covariations of traits underlying sorghum stem biomass production and quality and their regulations by water availability: Insight from studies at organ and tissue levels. GCB Bioenergy **11**, 444–462.

Main O, Jacquemot M-P, Griveau Y, *et al.* 2023. Precise control of water stress in the field reveals different response thresholds for forage yield and digestibility of maize hybrids. Frontiers in Plant Science **14**, 1142462.

Méchin V, Argillier O, Menanteau V, Barrière Y, Mila I, Pollet B, Lapierre C. 2000. Relationship of cell wall composition to in vitro cell wall digestibility of maize inbred line stems. Journal of the Science of Food and Agriculture **80**, 574–580.

Méchin V, Argillier O, Rocher F, Hébert Y, Mila I, Pollet B, Barriére Y, Lapierre C. 2005. In search of a maize ideotype for cell wall enzymatic degradability using histological and biochemical lignin characterization. Journal of Agricultural and Food Chemistry **53**, 5872–5881.

Mirhashemi SH, Panahi M. 2021. Investigation and prediction of maize water requirements in four growth stages under the influence of natural factors (Case study: Qazvin plain, Iran). Environmental Technology & Innovation **24**, 102062.

Molden D. 2007. *Water for Food Water for Life: A Comprehensive Assessment of Water Management in Agriculture*. Routledge.

Moore CE, Meacham-Hensold K, Lemonnier P, Slattery RA, Benjamin C, Bernacchi CJ, Lawson T, Cavanagh AP. 2021. The effect of increasing temperature on crop photosynthesis: from enzymes to ecosystems. Journal of Experimental Botany **72**, 2822–2844.

Moura JCMS, Bonine CAV, de Oliveira Fernandes Viana J, Dornelas MC, Mazzafera P. 2010. Abiotic and biotic stresses and changes in the lignin content and composition in plants. Journal of Integrative Plant Biology **52**, 360–376.

Néné-bi F, Turquin L, Konan S, Soro D, Ayolie K, Bléhou C, Kouadio J. 2022. Effects of Water Stress on the Agromorphological Parameters of Two New Maize (Zea mays L.) Lines (L36 and L71) Obtained from the Variety EV8728. European Scientific Journal, ESJ **18**, 120.

Nozière P, Sauvant D, Delaby L. 2018. *Alimentation des ruminants*. Versailles: Éditions Quae.

Osborne TM, Wheeler TR. 2013. Evidence for a climate signal in trends of global crop yield variability over the past 50 years. Environmental Research Letters **8**, 024001.

Peracchi LM, Panahabadi R, Barros-Rios J, Bartley LE, Sanguinet KA. 2024. Grass lignin: biosynthesis, biological roles, and industrial applications. Frontiers in Plant Science **15**, 1343097.

Perrier L, Rouan L, Jaffuel S, *et al.* 2017. Plasticity of Sorghum Stem Biomass Accumulation in Response to Water Deficit: A Multiscale Analysis from Internode Tissue to Plant Level. Frontiers in Plant Science **8**, 1516.

Peyrat J, Nozière P, Le Morvan A, Meslier E, Protin P-V, Carpentier B, Baumont R. 2016. *Prévoir la digestibilité et la valeur energétique du maïs fourrage: Guide des nouvelles références*. ARVALIS - Institut du végétal - INRA.

R Core Team. 2022. R: A language and environment for statistical computing. R Foundation for Statistical Computing, Vienna, Austria. URL https://www.R-project.org/. *in press*.

Ray DK, Gerber JS, MacDonald GK, West PC. 2015. Climate variation explains a third of global crop yield variability. Nature Communications **6**, 5989.

Reynolds M, Langridge P. 2016. Physiological breeding. Current Opinion in Plant Biology **31**, 162–171.

Riboulet C, Lefevre B, Dénoue D, Barrière Y. 2008. Genetic variation in maize cell wall for lignin content, lignin structure, p-hydroxycinnamic acid content, and digestibility in a set of 19 lines at silage harvest maturity. Maydica **53**, 11–19.

RStudio Team. 2022. RStudio: Integrated Development Environment for R. RStudio, PBC, Bostom, MA URL http://www.rstudio.com/. *in press*.

Salter PJ, Goode. 1967. Crop Responses to Water at Different Stages of Growth. Soil Science Society of America Journal **33**, iv–iv.

Santiago R, Barros-Rios J, Malvar RA. 2013. Impact of cell wall composition on maize resistance to pests and diseases. International Journal of Molecular Sciences **14**, 6960–6980.

dos Santos AB, Bottcher A, Kiyota E, Mayer JLS, Vicentini R, Brito M dos S, Creste S, Landell MGA, Mazzafera P. 2015. Water stress alters lignin content and related gene expression in two sugarcane genotypes. Journal of Agricultural and Food Chemistry **63**, 4708–4720.

Schindelin J, Arganda-Carreras I, Frise E, *et al.* 2012. Fiji: an open-source platform for biological-image analysis. Nature Methods **9**, 676–682.

Schlenker W, Roberts MJ. 2009. Nonlinear temperature effects indicate severe damages to U.S. crop yields under climate change. Proceedings of the National Academy of Sciences of the United States of America **106**, 15594–15598.

Schneider CA, Rasband WS, Eliceiri KW. 2012. NIH Image to ImageJ: 25 years of image analysis. Nature Methods **9**, 671–675.

Sen R, Karim N, Islam MdT, Rahman M, Adham AKM. 2019. Estimation of actual crop evapotranspiration and supplemental irrigation for Aman rice cultivation in the northern part of Bangladesh. Fundamental and Applied Agriculture **4**, 873–880.

Shao R, Yu K, Li H, Jia S, Yang Q, Zhao X, Zhao Y, Liu T. 2021. The effect of elevating temperature on the growth and development of reproductive organs and yield of summer maize. Journal of Integrative Agriculture **20**, 1783–1795.

Shu F, Jiang B, Yuan Y, Li M, Wu W, Jin Y, Xiao H. 2021. Biological Activities and Emerging Roles of Lignin and Lignin-Based Products—A Review. Biomacromolecules **22**, 4905–4918.

Spinoni J, Vogt JV, Naumann G, Barbosa P, Dosio A. 2018. Will drought events become more frequent and severe in Europe? International Journal of Climatology **38**, 1718–1736.

Surault F, Emile JC, Briand M, Barrière Y, Traineau R. 2005. Variabilité génétique de la digestibilité in vivo d'hybrides de maïs. Bilan de 34 années de mesures. 16.

Taube F, Vogeler I, Kluß C, Herrmann A, Hasler M, Rath J, Loges R, Malisch CS. 2020. Yield Progress in Forage Maize in NW Europe—Breeding Progress or Climate Change Effects? Frontiers in Plant Science **11**.

Tolera A, Sundstøl F. 1999. Morphological fractions of maize stover harvested at different stages of grain maturity and nutritive value of different fractions of the stover. Animal Feed Science and Technology **81**, 1–16.

Tolivia D, Tolivia J. 1987. Fasga: A new polychromatic method for simultaneous and differential staining of plant tissues. Journal of Microscopy **148**, 113–117.

Turc O, Tardieu F. 2018. Drought affects abortion of reproductive organs by exacerbating developmentally driven processes via expansive growth and hydraulics. Journal of Experimental Botany **69**, 3245–3254.

Vermorel, M., Coulon, J. B., Journet, M. 1987. Révision du système des unités fourragères (UF). Bulletin technique du CRZV Theix, 9–18.

Virlouvet L, El Hage F, Griveau Y, *et al.* 2019. Water Deficit-Responsive QTLs for Cell Wall Degradability and Composition in Maize at Silage Stage. Frontiers in Plant Science **10**, 488.

Visualizations with statistical details: The `ggstatsplot' approach. *in press*.

Wei T, Simko V. R package 'corrplot': Visualization of a Correlation Matrix (Version 0.92). Available from https://github.com/taiyun/corrplot. *in press*.

Van der Weijde T, Huxley LM, Hawkins S, Sembiring EH, Farrar K, Dolstra O, Visser RGF, Trindade LM. 2017. Impact of drought stress on growth and quality of miscanthus for biofuel production. GCB Bioenergy **9**, 770–782.

Welcome to the Tidyverse. *in press*.

Wickham H. 2016. *ggplot2: Elegant Graphics for Data Analysis*. Cham: Springer International Publishing : Imprint: Springer.

Wickham H, François R, Henry L, Müller K. 2022. dplyr: A Grammar of Data Manipulation. https://dplyr.tidyverse.org, https://github.com/tidyverse/dplyr. *in press*.

Zhang Y, Culhaoglu T, Pollet B, Melin C, Denoue D, Barrière Y, Baumberger S, Méchin V. 2011. Impact of Lignin Structure and Cell Wall Reticulation on Maize Cell Wall Degradability. Journal of Agricultural and Food Chemistry **59**, 10129–10135.

Zhang H, Han M, Comas LH, DeJonge KC, Gleason SM, Trout TJ, Ma L. 2019. Response of Maize Yield Components to Growth Stage-Based Deficit Irrigation. Agronomy Journal **111**, 3244–3252.

Zhang Y, Legay S, Barrière Y, Méchin V, Legland D. 2013. Color Quantification of Stained Maize Stem Section Describes Lignin Spatial Distribution within the Whole Stem. Journal of Agricultural and Food Chemistry **61**, 3186–3192.

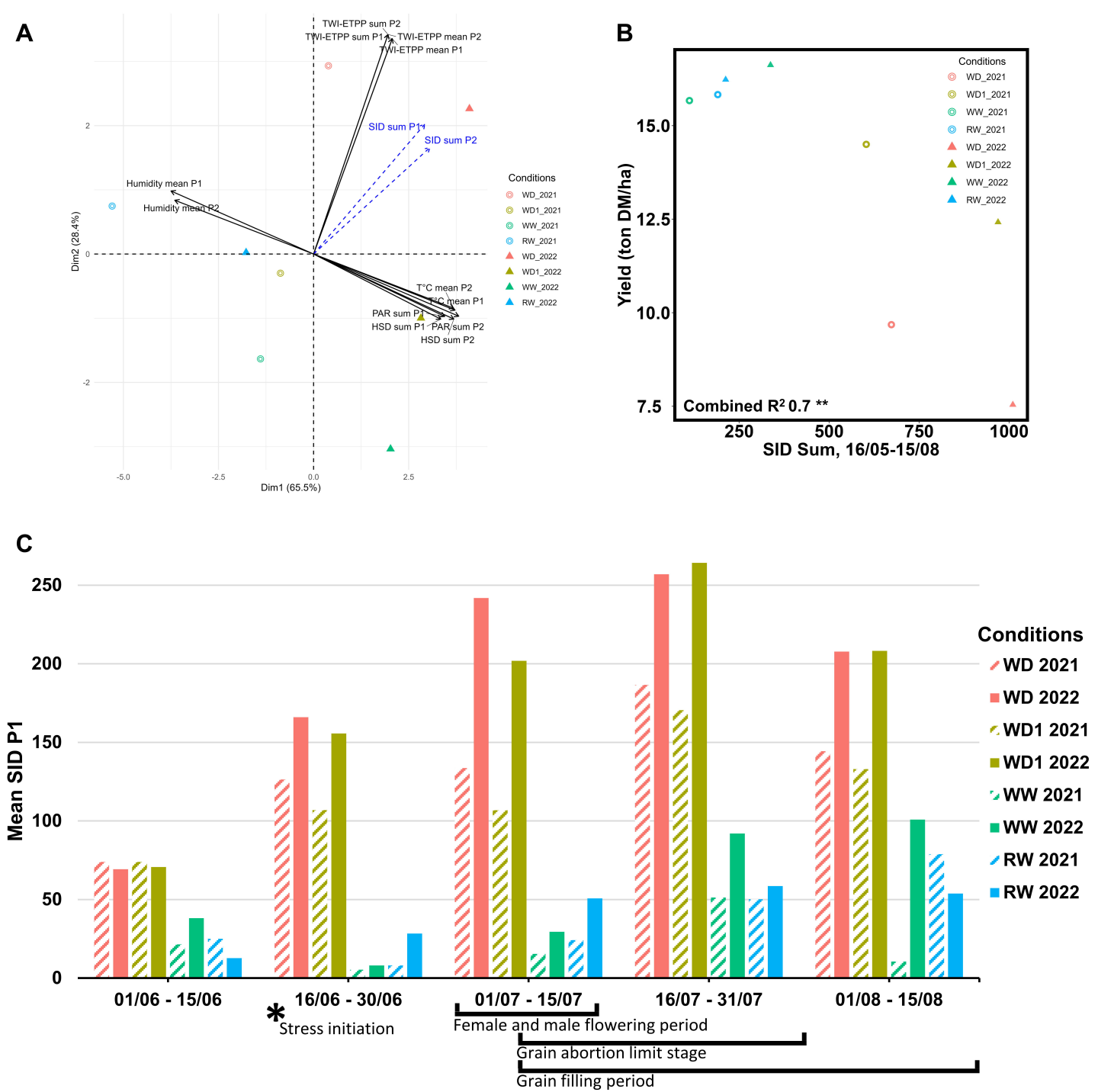

<u>Figure 1:</u> Analysis of climatic, environmental and stress index data across the main growth periods. (A) Distribution of the main environmental and climatic variables, alongside SID variables projected as spectator variables on the first two principal components. **(B)** Linear correlation between the SID sum between the 16th of May to the 15th of August to overall whole plant yield in ton DM/ha at harvest. **(C)** Mean SID values per half month period from the 1st of June to the 15th of August for the eight different conditions. Main physiological stages, including stress initiation and both flowering and grain-related periods are added below.

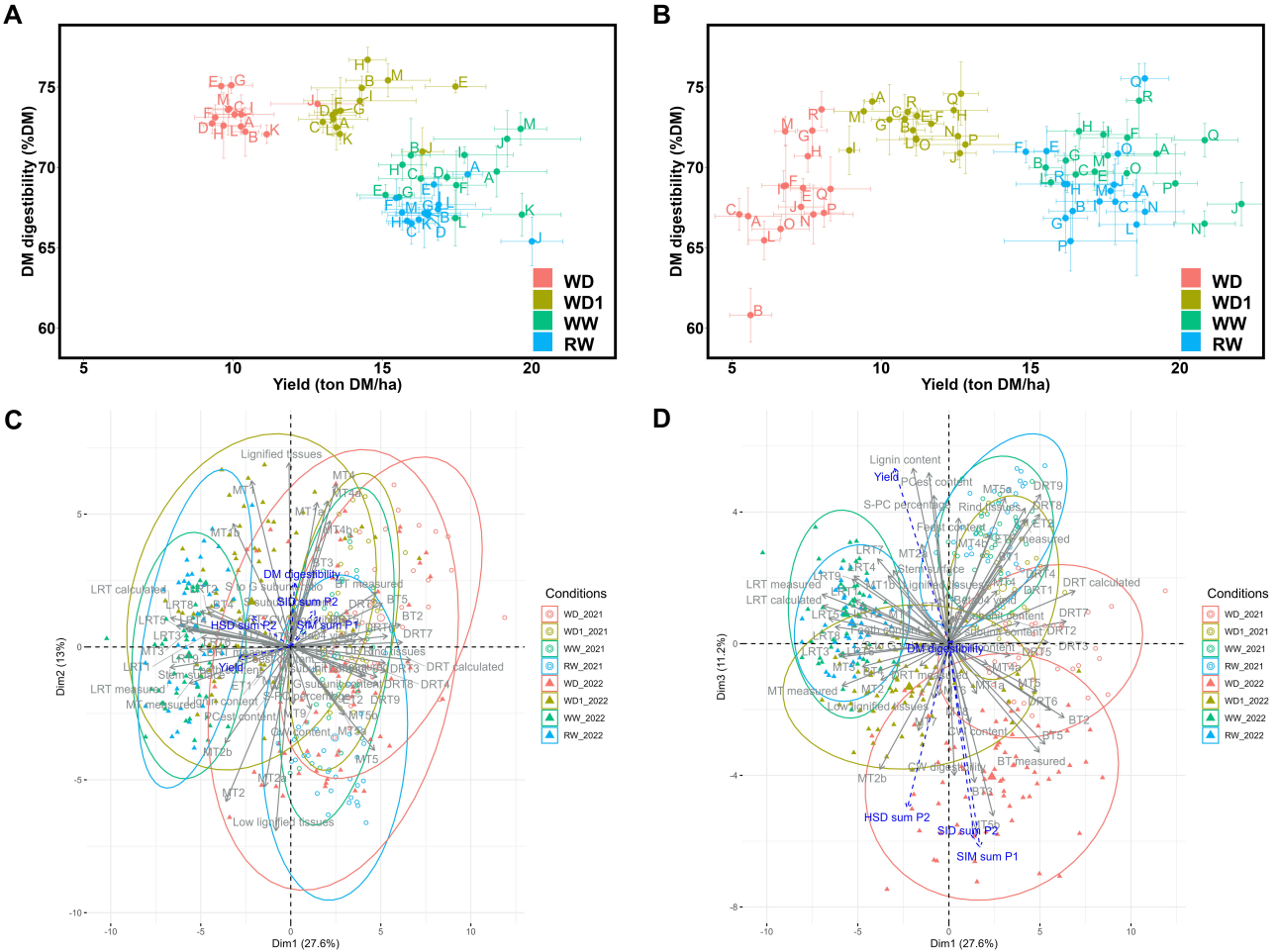

Figure 2: Impact of water deficit stress levels across 2021 and 2022 on agronomic trait response and variability. (A) DM digestibility to yield per variety under the four environmental conditions in 2021 and in 2022 **(B)**. **(C)** Combined projection of the contribution of each trait and each hybrid variety and each growing condition in the first two principal components (27.6% and 13% of the global variance, respectively). **(D)** Combined projection of the contribution of each trait and each hybrid variety and each growing condition in the first two principal components (27.6% and 11.2% of the global variance, respectively). In both PCAs, ellipses represent the area occupied by 95% of the hybrids for each treatment, with spectator traits in blue.

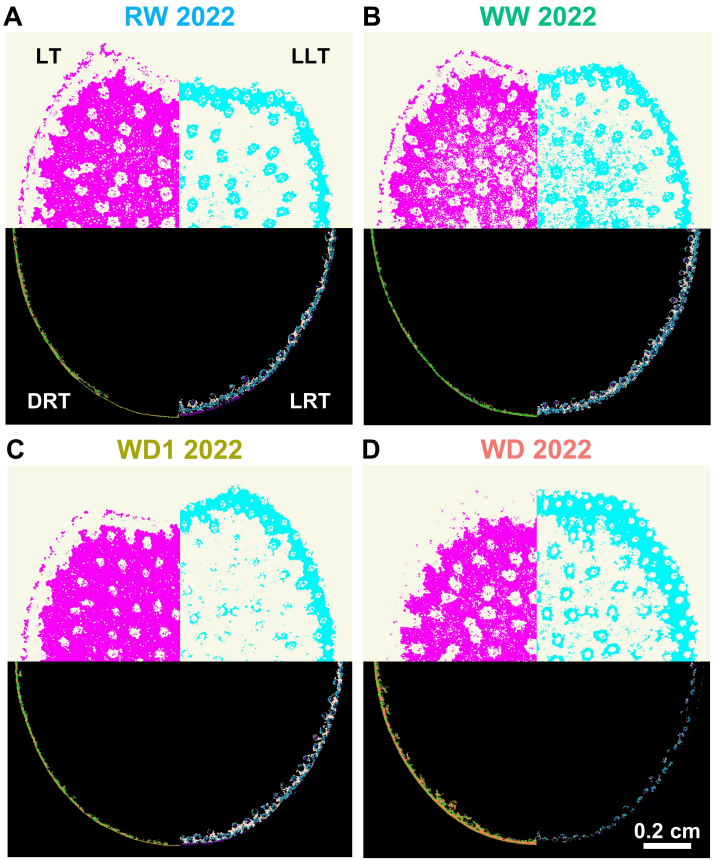

<u>Figure 3:</u> Impact of water deficit intensity on tissular distribution of biochemical traits. Distribution of the four main summarized tissue types in variety H for the humid (A-B), moderate (C) and severe (D) stress conditions. In each image, Lignified Tissues (**LT**) are presented in the top left quarter while Low Lignified Tissues (**LLT**) are opposite on the top right quarter. On the bottom left quarter, calculated Dark Rind Tissues (**DRT**) are placed opposite Light Rind Tissues (**LRT**) in the bottom right quarter. Tissue types are represented in **(A)** and image scale in **(D)**. All images are set at the same scale.

	Step Wise Selection for CW digestibility							
Group	**Step**	**Introduced Trait**	**Trait Pearson correlation**	**Partial R^2**	**Model R^2**	**RMSE**	**Model Coefficient**	**B vs H**
Year results	**2021 & 2022 combined**							
	1	Lignin content (%CWR)	-0,57	0,32	0,32	2,6	-1,733	***100% B***
	2	β04 yield (µmol/g lignin content)	-0,37	0,14	0,46	2,18	-0,005	
	3	Feest (mg/g CWR)	*ns*	0,07	0,53	2,05	0,949	
	4	PCest (mg/g CWR)	-0,6	0,04	0,57	1,96	-0,289	
	2021 separated							
	1	Lignin content (%CWR)	-0,76	0,57	0,57	1,94	-1,634	
	2	PCest (mg/g CWR)	-0,74	0,09	0,66	1,72	-0,68	
	3	MT2b (%ICS)	0,19	0,06	0,72	1,57	0,192	
	4	β04 yield (µmol/g lignin content)	-0,4	0,11	0,83	1,16	-0,003	
	2022 separated							
	1	Lignin content (%CWR)	-0,45	0,19	0,19	2,82	-1,595	***100% B***
	2	G subunit (µmol/g lignin content)	-0,36	0,19	0,38	2,48	-0,02	
	3	Feest (mg/g CWR)	*ns*	0,05	0,43	2,39	0,846	
	4	PCest (mg/g CWR)	-0,46	0,04	0,47	2,33	-0,418	
Humid conditions	**RW 2021**							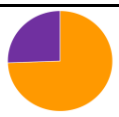
	1	PCest (mg/g CWR)	-0,69	0,47	0,47	1,76	-1,768	
	2	MT5b (%ICS)	0,41	0,17	0,64	1,43	0,043	
	3	S/G subunit ratio	*ns*	0,17	0,81	1,03	38,079	
	4	MT3 (%ICS)	*ns*	0,05	0,86	0,88	-34,633	
	RW 2022							***100% H***
	1	MT7 (%ICS)	*ns*	0,07	0,07	2,63	-17,936	
	WW 2021							
	1	S subunit (µmol/g lignin content)	-0,89	0,78	0,78	0,99	-0,064	***100% B***
	2	H subunit (µmol/g lignin content)	*ns*	0,14	0,92	0,62	0,312	
	WW 2022							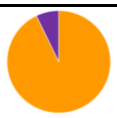
	1	Lignin content (%CWR)	-0,67	0,44	0,44	2,33	-1,395	
	2	Feest (mg/g CWR)	0,48	0,25	0,69	1,85	1,758	
	3	PCest (mg/g CWR)	-0,69	0,09	0,78	1,57	-0,694	
	4	MT7 (%ICS)	*ns*	0,06	0,84	1,38	34,602	
Moderate to severe stress conditions	**WD1 2021**							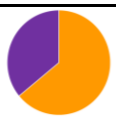
	1	Lignin content (%CWR)	-0,7	0,49	0,49	1,62	-2,839	
	2	DRT3 (%ICS)	-0,6	0,18	0,67	1,32	-9,136	
	3	MT5a (%ICS)	-0,59	0,07	0,74	1,17	-0,089	
	4	LRT6 (%ICS)	*ns*	0,06	0,8	1,05	119,14	
	WD 2021							
	1	Lignin content (%CWR)	-0,6	0,36	0,36	1,32	-1,547	
	2	DRT4 (%ICS)	-0,48	0,21	0,57	1,09	-16,496	
	3	Feeth (mg/g CWR)	*ns*	0,06	0,63	1,03	-0,123	
	4	DRT2 (%ICS)	-0,36	0,03	0,66	0,99	-86,508	
	5	S-PC (%)	-0,46	0,15	0,81	0,83	-4,682	
	WD1 2022							
	1	Feest (mg/g CWR)	*ns*	0,08	0,08	2,44	3,638	
	2	PCest (mg/g CWR)	*ns*	0,14	0,22	2,4	-3,253	
	3	MT4b (%ICS)	-0,27	0,1	0,32	2,17	-0,125	
	4	BT5 (%ICS)	*ns*	0,08	0,4	2,07	6,322	
	5	Medullary Tissues (%ICS)	*ns*	0,08	0,48	1,96	0,639	
	6	BT3 (%ICS)	*ns*	0,06	0,54	1,86	-3,699	
	7	LRT2 (%ICS)	*ns*	0,06	0,6	1,75	69,17	
	8	LRT1 (%ICS)	*ns*	0,06	0,66	1,62	-327,266	
	9	S/G subunit ratio	*ns*	0,16	0,82	1,24	-7,949	
	6	MT2b (%ICS)	*ns*	0,08	0,89	0,63	0,21	
Severe stress condition	**WD 2022**							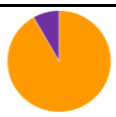
	1	S-PC (%)	-0,77	0,59	0,59	2,07	-16,168	
	2	Lignin content (%CWR)	*ns*	0,13	0,72	1,75	-1,925	
	3	Feest (mg/g CWR)	*ns*	0,06	0,78	1,57	1,794	
	4	MT5a (%ICS)	-0,27	0,07	0,85	1,33	-0,155	

Figure 5: Biochemical and histological trait relation to CW digestibility and regression model construction.
Conditions are listed progressively depending on their level of stress intensity. Introduced traits are listed depending on the step they were introduced into the model. Their respective direct relation to CW digestibility is then evaluated via Pearson correlation. This is followed by their individual contribution to the regression model, and then the overall model R square. Following this is then the model root mean square error (RMSE) and it's evolution depending on the introduced traits, and then the model coefficient for each trait. A pie chart then represents the contribution of both biochemical (Biochemistry, B) versus histological traits (Histology, H) traits within the indicated model, with the total being equal to the sum of both parts.

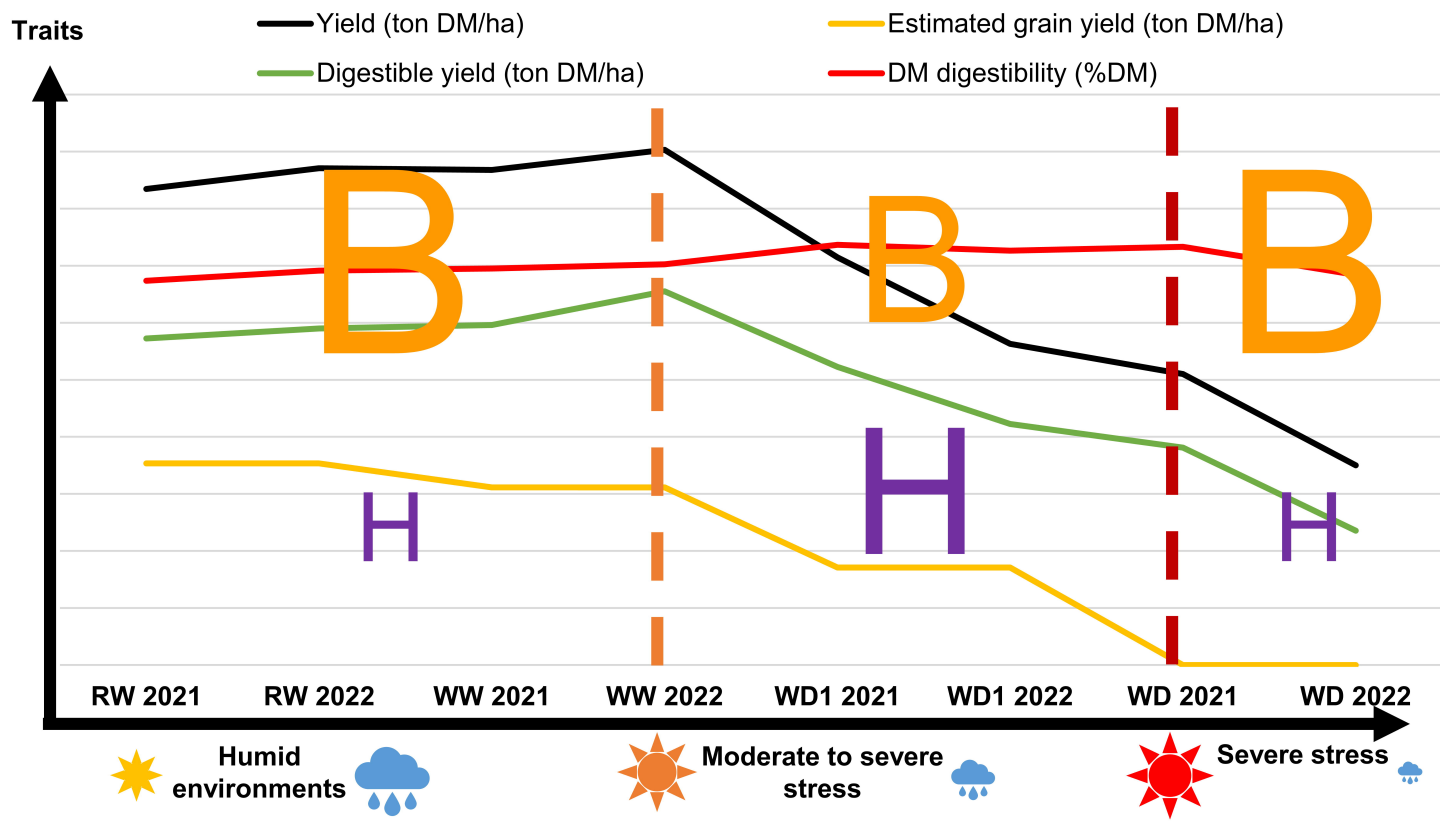

<u>Figure 6:</u> Model of forage maize digestibility response under progressively increasing water and heat stress intensity. Traits analysed at the mean level for the different Mauguio and Versailles conditions. Biochemistry (lignin content, *p*-coumaric and ferulic acid, lignin subunit and linkages yield) traits are abbreviated to "B", histology (lignin distribution) traits are abbreviated to "H", with their size reflecting their importance within the considered environmental stress level determined in Figure 5.